https://doi.org/10.5194/egusphere-2026-1205
Preprint. Discussion started: 11 March 2026


# Decadal predictions of wind, solar and compound power indicators to support the European renewable energy sector

Sara Moreno-Montes[1], Carlos Delgado-Torres[1], Matías Olmo[1], Sushovan Ghosh[1], Verónica Torralba[1], and Albert Soret[1]

[1]Barcelona Supercomputing Center (BSC), Barcelona, Spain

**Correspondence:** Sara Moreno-Montes (sara.moreno@bsc.es)

**Abstract.** Renewable energy production is strongly influenced by climate variability and change, making the energy sector sensitive to fluctuations on decadal timescales. Decadal climate predictions, which aim to forecast climate variability over the next few years, therefore offer potential value for anticipating near-term changes in wind and solar resources and supporting climate-informed energy planning. However, the predictive skill of decadal forecasts for energy-relevant indicators remains poorly quantified, which is crucial to know the potential usability of any forecast product.

This study evaluates the skill of decadal climate predictions over Europe for forecast years 1–3 using a multi-model ensemble from the Coupled Model Intercomparison Project Phase 6 (CMIP6) Decadal Climate Prediction Project (DCPP). We assess three energy-relevant indicators: photovoltaic potential (PVpot), wind capacity factor (WCF), and a compound indicator describing the number of energy drought days (NED), defined as days with inefficient production from both wind and solar resources. The skill is evaluated against the ERA5 reanalysis, and the added value of the model initialization is estimated by comparing the decadal predictions against the non-initialized historical forcing simulations. PVpot exhibits the highest and most spatially homogeneous skill for annual, spring and summer aggregations, closely reflecting the high predictability of surface solar radiation. WCF shows low and spatially heterogeneous skill, consistent with the high intrinsic variability of wind. The compound NED indicator displays strong seasonal dependence: its predictability is largely controlled by solar conditions in high-radiation seasons and by wind in winter and autumn. Model initialization generally provides added value where historical simulations already show some skill, especially for PVpot, while its impact is lower for WCF. This work shows the specific seasons, regions and energy indicators for which decadal predictions can provide actionable climate information to support renewable energy applications.

## 1 Introduction

The renewable energy sector has gained increasing importance in Europe in recent years, with wind and solar representing a growing fraction of total electricity generation (Agency, 2022). Continued policy support and decarbonisation targets are expected to further accelerate this expansion in the coming decades (IEA, 2024). Renewable energy production depends strongly on variations in key climate variables such as near-surface air temperature, solar radiation or surface wind speed (Solomon, 2007), and ambitious deployment targets across Europe further highlight the need for climate-informed planning in the energy

https://doi.org/10.5194/egusphere-2026-1205
Preprint. Discussion started: 11 March 2026


sector (e.g., Ely et al., 2013; Gonzalez et al., 2019). While long-term climate projections are essential for strategic planning, and short-term forecasts support daily operations, the intermediate horizon of next years remains comparatively underexploited (Smith et al., 2019). Decadal climate predictions, which bridge the gap between seasonal forecasts and long-term projections, are emerging as a valuable tool for sectors that must adapt to both climate variability and climate change (Meehl et al., 2009; Boer et al., 2016). In the energy sector, such information could support infrastructure development, system resilience, and risk management decisions (Challinor et al., 2017; Commission, 2020). Despite this potential, the explicit integration of decadal climate information into wind and solar energy assessments remains limited, highlighting a gap between advances in decadal prediction science and their application in the renewable energy sector.

Previous studies have evaluated the forecast skill of decadal prediction systems for essential climate variables and extreme indices (Association et al., 2023; Delgado-Torres et al., 2022, 2023; World Meteorological Organization, 2024), and have also explored the role of statistical downscaling in improving regional skill (Moreno-Montes et al., 2026). In parallel, decadal forecasts have been applied to sector-specific climate services, including agriculture (Solaraju-Murali et al., 2022; Delgado-Torres et al., 2025), water management (Paxian et al., 2022), marine fisheries (Payne et al., 2022), and hydropower (Tsartsali et al., 2023), as well as multi-sector studies demonstrating the application of decadal predictions (Dunstone et al., 2022; Done et al., 2021). However, research on decadal climate services explicitly focused on the energy sector remains limited. Early assessments have reported regionally dependent skill for decadal predictions of wind-related variables, including near-surface wind speed and wind energy output, with skill often enhanced through downscaling approaches (Haas et al., 2015; Moemken et al., 2016). More recent work has highlighted relatively high skill for surface solar radiation, while wind speed skill remains generally low over Europe (Hutchins et al., 2025). By comparison, climate services for the energy sector have been more extensively explored at sub-seasonal to seasonal timescales (Clark et al., 2017; Torralba et al., 2017b; Bloomfield et al., 2021; Bett et al., 2022; Cionni et al., 2022; Lledó et al., 2022; Soret et al., 2026) and with long-term climate projections (Carvalho et al., 2021; Hou et al., 2021; Olmo et al., 2026).

In this study, we assess the skill of decadal predictions for energy-relevant indicators derived separately for solar and wind energy, and we further explore compound indicators that combine information from both sources. Compound events are particularly relevant because simultaneous deficits in multiple energy resources can exacerbate the risk of energy shortages and stress the energy system (Zscheischler et al., 2018; Otero et al., 2022). Analyzing each energy source independently allows us to characterize source-specific predictability, while the combined indicators capture the co-variability of wind and solar resources and its implications for energy system operations. Previous studies have shown that combining multiple renewable energy sources, particularly wind and solar, can enhance system robustness by exploiting their temporal and spatial complementarity, and can support planning and balancing strategies in highly renewable energy systems (Heide et al., 2010; Monforti et al., 2014; Jerez et al., 2019; Kapica et al., 2024). Decadal predictions of compound hot-dry extreme events have been recently explored by Aranyossy et al. (2025). However, to the best of our knowledge, an assessment of the forecast quality of decadal predictions for compound power indicators remains lacking, limiting the understanding of their utility for energy systems planning and risk management over multi-year timescales.

https://doi.org/10.5194/egusphere-2026-1205
Preprint. Discussion started: 11 March 2026


This study is organized as follows. Section 2 describes the datasets used to compute the indicators including observation-based reference datasets, decadal predictions and historical simulations. Section 3 presents the methodology to compute the solar- and wind-based indicators, and compound indicators. Section 4 presents the results together with the discussion and a comparison with previous studies. Finally, Section 5 summarizes the main findings, discussing their implications and suggesting directions for future research.

## 2 Data

In this study, five different decadal forecast systems contributing to the Decadal Climate Prediction Project (DCPP; Boer et al., 2016) of the Coupled Model Intercomparison Project Phase 6 (CMIP6; Eyring et al., 2016), are used. In addition, to analyze the impact of initialization, the indicators are computed for the three corresponding CMIP6 non-initialized historical forcing simulation models. The main characteristics of the DCPP forecast systems and the historical simulation models, including ensemble size, spatial resolutions, initialization months (for the DCPP-A), and references, are detailed in Table S1 of the Supplementary Material. Additionally, the ERA5 reanalysis (Hersbach et al., 2020) dataset is used as the observation-based reference. This observational reference has been selected taking into account its temporal and spatial coverage and because it is widely used by the energy community (Ramon et al., 2024).

Depending on the energy source, different temporal resolutions and variables are used. For solar energy indicators, daily values of surface downwelling shortwave radiation (RSDS), near-surface air temperature (TAS), and surface wind speed (SFCWIND) are employed. For wind energy indicators, instantaneous 6-hourly surface wind (6h-SFCWIND) data are used. As sub-daily data are required to compute the wind indicators (Lledó et al., 2022), the number of available models is reduced.

Start dates from 1960 to 2016 are used for decadal predictions, focusing the analysis on forecast years 1–3. Therefore, to match the period, we use the ERA5 data, as well as the historical forcing simulations concatenated with the scenario ssp245 (O'Neill et al., 2016), during 1961–2019. Historical simulations provide data until 2014, and ssp245 is used for the rest of the years (2015-2019).

The analysis focuses on Europe, defined by the spatial domain spanning longitudes 30°W–12°E and latitudes 35°N–65°N.

## 3 Methodology

To ensure consistency across datasets, variables from all model simulations are first interpolated to the ERA5 grid (0.25°). To calculate wind energy indicators, since decadal prediction systems and historical simulations do not provide wind speeds at hub height, 6h-SFCWIND data from both the reference dataset and the model simulations are converted to wind speeds at 100m (6-hWIND). A representative hub height of 100m is assumed for modern wind turbines (Wiser et al., 2023). To estimate hub height winds from surface winds, a power law is applied (Brower, 2012), using a shear exponent of $\alpha = 0.143$ (Touma, 1977) over land and $\alpha = 0.11$ over water (International Electrotechnical Commission: IEC, 2005), under the assumption of neutral atmospheric stability.

https://doi.org/10.5194/egusphere-2026-1205
Preprint. Discussion started: 11 March 2026


In addition, ERA5 wind speeds are adjusted using the Global Wind Atlas (GWA) to better represent long-term mean conditions at hub height. Figure S1 shows the climatological ratio between ERA5 and GWA mean 6-hWIND over 1961–2019, which is applied as a pointwise correction to the ERA5 data. This ensures a more realistic representation of wind resources while preserving the temporal variability from ERA5 (Lledó et al., 2022).

After interpolation and wind-specific corrections, all decadal predictions and historical simulations are calibrated against ERA5 using Empirical Quantile Mapping (EQM; Panofsky and Brier, 1958). EQM maps the quantiles (percentiles) of the modelled data to the observed ones without assuming any underlying distribution and then it corrects the model biases. Calibration is performed per forecast year and member for decadal predictions, and per calendar year and member for historical simulations. In both cases, a 30-day moving window centered on the target date is applied to remove short-term fluctuations and preserve seasonality while ensuring a sufficient sample size. A leave-one-year-out cross-validation is used to prevent overfitting and artificial skill inflation (Elsner and Schmertmann, 1994). For 6-hWIND, the calibration is performed separately for each time of the day, since wind distributions differ markedly across the diurnal cycle (Kalverla et al., 2019; Weide Luiz and Fiedler, 2022).

The calibrated climate variables are then used to compute the energy indicators. All indicators are calculated separately for each climatological season and for the whole year. We define three indicators: photovoltaic potential (PVpot) for solar energy, capacity factor for wind energy (WCF), and the Number of Energy Droughts (NED). The intermediate metric Number of Effective days (Neff) is first computed for each resource and subsequently combined to derive NED. Indicators are computed for each forecast system and for the ERA5 reanalysis, which we use as a reference to assess predictive performance. Results for wind-related indicators are analyzed over land and over sea-adjacent regions, as both onshore and offshore wind resources are of practical interest for current and future wind energy deployment.

Following previous studies (Mavromatakis et al., 2010; Jerez et al., 2015), PVpot is computed as a dimensionless metric that combines RSDS, TAS and SFCWIND to represent the performance of photovoltaic cells under ambient environment. PV power generation at a specific location is determined by multiplying PVpot with the nominal installed capacity of that location. The PVpot is mainly driven by RSDS, with adjustments for TAS, which lowers module efficiency at higher temperatures (Radziemska, 2003), and SFCWIND, which can partially offset thermal losses through convective cooling. Although the equation S1 provides as a unitless quantity, in this study they are converted to percentage values to facilitate the visual interpretation. Even though daily inputs are less precise than hourly due to aggregation, they keep seasonal and annual errors small and avoid the much larger biases seen with monthly data (Müller et al., 2019; Bett and Thornton, 2016).

WCF is defined as the ratio between the energy actually produced and the energy that would be generated if the turbine operated continuously at its rated power. WCF depends on the turbine's power curve, which varies by turbine type and site conditions; the standard power curves defined in IEC 61400-1 are shown in Figure S2. In this study IEC Class I turbine is adopted as a common reference, as a sensitivity analysis presented no notable differences among the skill performance of the different turbines (not shown). Given the high temporal resolution of turbine power curves and their strong nonlinearity, the use of 6-hourly wind data reduces aggregation bias. Although daily means are often adequate (MacLeod et al., 2018), sub-

https://doi.org/10.5194/egusphere-2026-1205
Preprint. Discussion started: 11 March 2026


daily data better preserves variability and yields more accurate WCF estimates (Lledó et al., 2022). WCF is derived using the R-based CSIndicators package (Pérez-Zanón et al., 2023).

PVpot and WCF are defined differently, so their absolute values should not be compared across energy sources. To enable a meaningful cross-resource comparison, Neff is defined as the number of days meeting efficiency-related thresholds, providing a common performance indicator with direct operational relevance.

For solar energy production, Neff efficiency thresholds are defined using a minimum RSDS and a maximum cell temperature (Tcell: Chenni et al. (2007)). The RSDS threshold is based on the concept of peak sun hours (PSH), defined as the equivalent number of hours per day with an irradiance of 1000 $\mathrm{W\,m^{-2}}$ (Duffie and Beckman, 1980). A commonly used lower limit for meaningful PV generation is 5 PSH per day, which corresponds to a daily mean RSDS of 208 $\mathrm{W\,m^{-2}}$ (Ghosh et al., 2022). Since higher TAS increases Tcell and reduces PVpot, an upper operating threshold of Tcell = 45 °C is applied (see equation S2), at which the PV module works at 90% of its rated-efficiency and above the threshold it progressively declines PV generation (Ghosh et al., 2024).

For wind energy, Neff is defined using both operational and performance criteria. Although IEC Class I turbines operate between cut-in (2 $\mathrm{ms^{-1}}$) and cut-out (25 $\mathrm{ms^{-1}}$) wind speeds, winds just above cut-in typically yield little energy production. Therefore, effectiveness is defined using a minimum threshold of WCF $\geq$ 25%, which excludes periods of low-efficiency production and can be associated with economically relevant wind power generation (Boccard, 2009; Kealy et al., 2015). This threshold is translated into an equivalent minimum wind speed using the turbine power curve, and effective time steps are counted when wind speeds exceed this value while remaining below cut-out. To ensure consistency with solar indicators, 6-hourly wind data are aggregated to daily values, defining a day as effective when at least 3 of 4 time steps meet the threshold (Figure S3).

Based on the effective number of days in which any energy source can operate efficiently, we define the combined indicator NED, which corresponds to the number of days when neither source produces efficiently. Besides, the Neff for each energy source (solar-Neff and wind-Neff) and for both (both-Neff) are calculated.

Once the corresponding indicators are calculated for each forecast year, the forecast years 1-3 are averaged in order to obtain a mean value over the entire forecast period for each forecast system. To ensure a consistent comparison with decadal predictions, a rolling mean with a window length equal to the number of forecast years (3) is applied to the historical simulations and ERA5 time series. Subsequently, multi-model ensembles are constructed for decadal predictions (DCPP) and historical simulations (HIST) following the multi-model mean approach (Delgado-Torres et al., 2022).

The performance of the DCPP is evaluated against the ERA5 reanalysis using the Anomaly Correlation Coefficient (ACC; Wilks, 2011. ACC ranges from -1 (perfect inverse correlation) to 1 (perfect correlation). A one-sided t-test is applied to determine if ACC values differ significantly from zero (Wilks, 2011). Following Storch and Zwiers (1999), the effective number of degrees of freedom is used to account for autocorrelation in the time series. To assess the impact of initialization, the residual correlation (ResCorr; Smith et al., 2019) between the DCPP and ERA5 is calculated relative to the HIST. Positive values of ResCorr indicate that decadal predictions can capture more observed variability that is not already captured by the historical simulations.

https://doi.org/10.5194/egusphere-2026-1205
Preprint. Discussion started: 11 March 2026


Finally, after computing the indicators for each grid point, a regionalization is applied to analyze trends and correlations at the regional scale. For each sub-region, indicators are first spatially area-weighted averaged to obtain a single representative time series, from which regional trends, correlations and ResCorr are calculated. This step is motivated by the known contribution of externally forced trends and low-frequency variability to decadal prediction skill in some variables (e.g. van Oldenborgh et al., 2012), and allows us to assess how long-term changes influence the estimated predictability. Europe is divided in seven sub-regions (Figure S4), following the regionalization of Priestley et al. (2024): Iberia, Western Europe, Mediterranean, Central Europe, Eastern Europe, Scandinavia, Great Britain and Ireland.

## 4 Results and discussion

The results are presented in three separate sections for each indicator: PVpot, WCF, and NED. In each section, the ACC between the DCPP of the indicator and ERA5 and the ResCorr between the DCPP and ERA5 relative to HIST are shown for the annual mean and individual seasons. The annual means provide an integrated measure of performance and reduce high-frequency variability, helping to highlight low-frequency signals relevant at decadal timescales. This information is usually required by energy stakeholders for planning the year ahead. Seasonal means allow the identification of season-dependent predictability which can be relevant for energy deployment. The ACC between the DCPP of the variables used to calculate the indicators (RSDS, TAS and SFCWIND) and ERA5 are presented in Figure S5.

### 4.1 Photovoltaic potential (PVpot)

The climatology of PVpot (S6a–e) shows higher values over southern Europe than at higher latitudes, reflecting the meridional gradient in solar irradiance, in line with previous studies (e.g. Šúri et al., 2007; Castillo et al., 2016). The associated interannual standard deviation is low across the domain (S6f–j), indicating that PVpot variability is small and largely controlled by mean climatological conditions.

Figure 1a-e shows the ACC between DCPP and ERA5 of PVpot for the annual mean and each season. The annual mean (Figure 1a) and JJA (Figure 1d) show the highest fractions of significant area, with positive skill over most of the region, except in parts of the UK, southern Europe and Scandinavia. In MAM (Figure 1c), the percentage of significant area is lower than in the annual mean and JJA, although the skill patterns are similar. This reduction is mainly due to northern Europe and parts of Iberia, where MAM skill is generally non-significant. On the other hand, DJF (Figure 1b) shows the lowest fraction of significant points, with significant skill only over parts of Iberia and Italy. ACC values during the SON season (Figure 1e) are significant in regions along the Atlantic coast and parts of Poland and the Baltic countries. Across all seasons, skill tends to be lower in mountainous regions, particularly over the Alps.

https://doi.org/10.5194/egusphere-2026-1205
Preprint. Discussion started: 11 March 2026


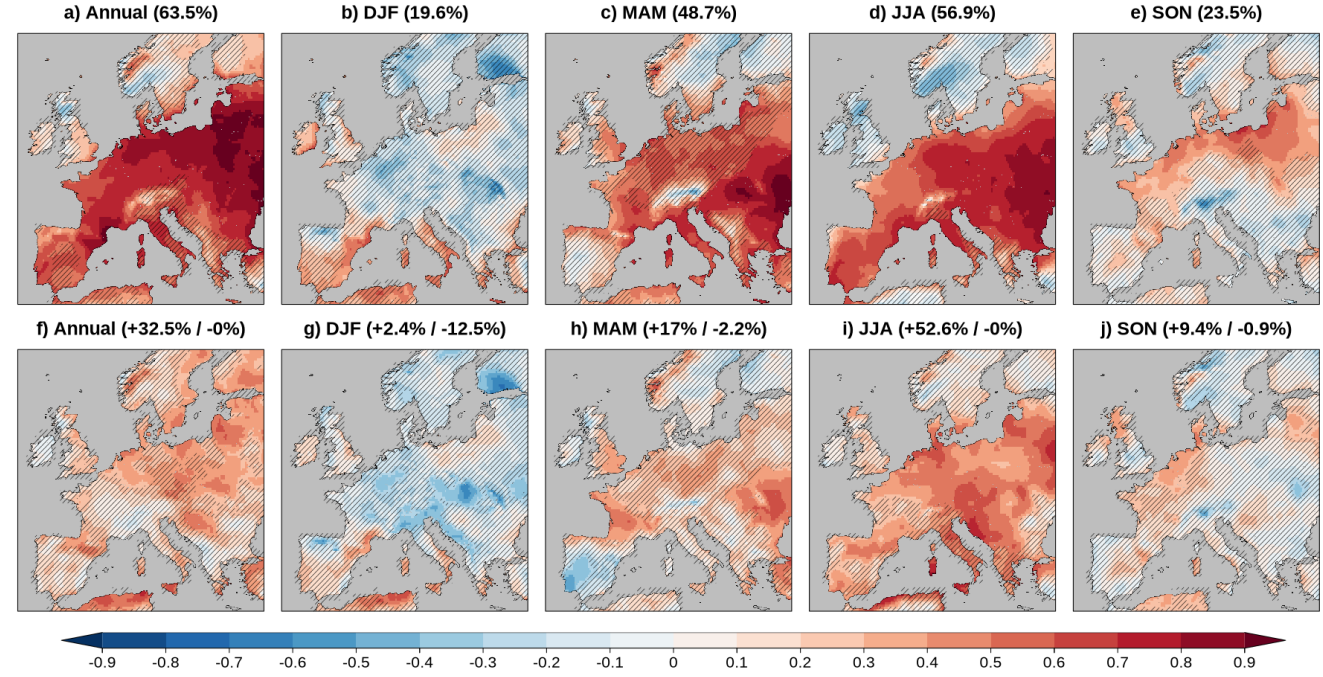


**Figure 1.** First row: ACC of DCPP of solar PVpot for the annual mean (a) and seasonal means (b–e) for forecast years 1–3. The percentages of significant grid points are indicated in brackets, and hatched regions denote non-significant correlations. Second row: ResCorr between DCPP and ERA5 relative to the HIST for the annual mean (f) and seasonal means (g–k). Percentages indicate the fractions of significantly positive (red) and significantly negative (blue) values. Positive (negative) ResCorr indicates higher (lower) skill for DCPP compared to HIST. Correlations are computed against ERA5 during the 1961-2019 period, and statistical significance is assessed using a one-sided t-test at the 95% confidence level, accounting for time-series autocorrelation.

Although the percentage of significant grid points is slightly lower for PVpot than for its main driver RSDS (Figure S5a-e), both variables show very similar spatial skill patterns. The reduction in PVpot skill relative to RSDS is more noticeable over southern Europe in the annual mean (Figure S5a and Figure 1a), over parts of central Europe in MAM (Figure S5c and Figure 1c), and over Iberia in SON (Figure S5e and Figure 1e). This loss of skill reflects the fact that PVpot is not only driven by RSDS but is also modulated by TAS and, with a smaller contribution, by SFCWIND. While TAS generally shows high and spatially homogeneous skill across most seasons (except in DJF; Figure S5g), and SFCWIND exhibits weaker and more heterogeneous skill (Figure S5k–o), their combined effect slightly decreases the overall PVpot predictability compared to RSDS alone.

The seasonal contrast in skill suggests a link with large-scale atmospheric conditions. Skill is higher in JJA and MAM, when more persistent radiative conditions typically dominate, and lower in DJF and in mountainous regions, when variability is stronger. However, these relationships are not spatially uniform and should be interpreted cautiously. Besides, the similarity between the annual and JJA skill patterns reflects the dominant contribution of high-radiation seasons to the annual PVpot signal. Since PVpot is strongly controlled by RSDS, and solar irradiance peaks during spring and summer, the annual mean

https://doi.org/10.5194/egusphere-2026-1205
Preprint. Discussion started: 11 March 2026


largely integrates the predictability of these seasons. In addition, annual averaging reduces short-term variability and increases signal-to-noise ratios, resulting in higher predictability and thus higher skill values.

Few studies have assessed decadal predictability for solar-energy indicators. Hutchins et al. (2025) have reported high summer skill for RSDS over southern and central Europe, broadly consistent with our results. They have also identified additional winter predictability using a NAO-based approach, which is not captured when evaluating PVpot from the multi-model ensemble. Focusing on seasonal predictions, Bett et al. (2022) have found higher predictability for RSDS in summer and lower in winter, in line with the seasonal contrast observed here for decadal predictions.

The added value of the DCPP relative to the HIST is assessed using the ResCorr (Figure 1f–j), and the ACC between HIST and ERA5 is shown in Figure S7. In the annual mean (Figure 1f) and JJA (Figure 1i), ResCorr is significantly positive over large parts of the domain, indicating that model initialization enhances PVpot skill relative to historical simulations. In these seasons, HIST skill is already generally high (Figure S7a,d), so initialization mainly amplifies existing positive skill. In DJF (Figure 1g), ResCorr exhibits localized negative values, indicating reduced skill in some regions. On the other hand, DCPP skill (Figure 1b) is lower than HIST skill (Figure S7b) in areas such as southern Iberia or the Alps. During the transition seasons, MAM and SON (Figure 1h,j), positive ResCorr values appear only in specific regions, mainly over eastern Europe and parts of the Atlantic coast for MAM and over northern Atlantic regions for SON, again corresponding to areas where HIST already exhibits positive skill (Figure S7c,e). Overall, initialization mainly enhances PVpot skill where historical simulations already exhibit predictability.

Figure 2 summarizes the regional behaviour of PVpot long-term trends across the seven European sub-regions (Figure S2), showing ERA5 trends (a), DCPP trends (b), their correlations (c), and their ResCorr respect the HIST (d) for the annual mean and each season. For Iberia, Western Europe, Mediterranean, Central Europe, and Eastern Europe, at the annual mean and during MAM and JJA, both datasets show positive significant trends, which are accompanied by significantly positive correlations. In DJF and SON, ERA5 trends in these regions are often weak or non-significant, while DCPP trends remain significantly positive, leading to generally low and non-significant correlations. Some exceptions to this behaviour occur (Iberia in DJF, Western Europe in SON, and Eastern Europe in SON), where better agreement between trends results in significant correlations. For Scandinavia and Great Britain and Ireland, trends generally disagree and correlations are low, with a few exceptions (Scandinavia in the annual mean and SON and Great Britain and Ireland in MAM), although significant correlations are limited to the the annual mean in Scandinavia and MAM in Great Britain and Ireland. Overall, these results highlight the strong link between trend agreement and the skill of decadal predictions.

https://doi.org/10.5194/egusphere-2026-1205
Preprint. Discussion started: 11 March 2026


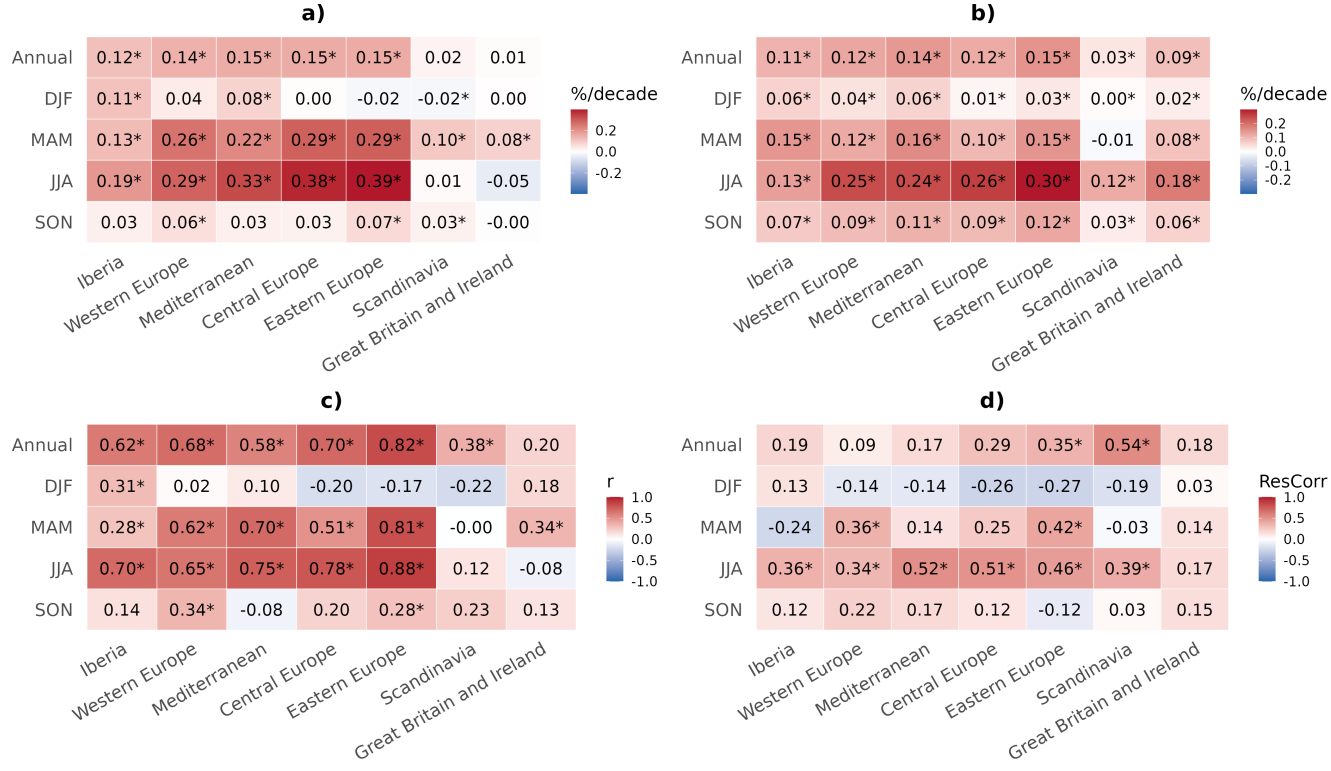


**Figure 2.** PVpot trends derived from ERA5 for years 1961-2019 with a three years rolling mean (a) and from the DCPP for the start dates 1960-2016 for over forecast years 1–3 (b), the correlation between ERA5 and DCPP (c), and the ResCorr between DCPP and ERA5 respect HIST (d) shown for the annual mean and for each season across the seven european sub-regions (Figure S4). Statistically significant trends and correlations at the 95% confidence level are marked with an asterisk.

PVpot trends follow similar patterns to those from RSDS (Figure S8a-b) for both ERA5 and DCPP, showing again that the variable is the main driver of the indicator. TAS trends (Figure S8c-d) are significantly positive in all the seasons and regions for both datasets, which are not aligned with the PVpot values.

ResCorr regional patterns (Figure 2d) show that in regions and seasons where correlations are significantly positive (Figure 2c), ResCorr values are generally also positive, although they are only significant in JJA for most regions, in Western and Eastern Europe during MAM, and in Eastern Europe and Scandinavia for the annual mean. This indicates that not all the skill shown in Figure 2c is explained by the similar trends of ERA5 (Figure 2a) and DCPP (Figure 2b) alone. Initialization adds additional skill beyond the externally forced signal in these cases. In DJF, ResCorr values are not significant in any region, indicating that initialization does not add skill beyond what is captured by the HIST. In SON, ResCorr values are mostly positive but small, suggesting that initialization provides a limited additional contribution compared to the forced trend. In summary, when ERA5 and DCPP trends agree, part of the skill is linked to the common trend, but initialization can still

https://doi.org/10.5194/egusphere-2026-1205
Preprint. Discussion started: 11 March 2026


enhance predictability in all the regions, particularly in JJA. On the other hand, when trends have opposite signs and correlations are non-significantly positive, ResCorr values are also non-significant.

The strong contribution of long-term trends to significant skill has been identified in several studies for decadal predictions (Meehl et al., 2009; Suckling et al., 2017) and historical simulations (Donat et al., 2023). Some studies have applied approaches to reduce model drift or systematic errors (Kharin et al., 2012), and others have shown that the skill of TAS is substantially reduced after removing the forced trend, whereas precipitation skill is less affected (Bellucci et al., 2015; Delgado-Torres et al., 2022). However, removing the trend may also influence forecast reliability and modify the balance between externally forced and internally driven variability (Corti et al., 2012; Smith et al., 2012). Rather than adopting a single approach, we explicitly present both perspectives. The ACC quantifies the total predictive skill, including the contribution from externally forced trends, which are themselves relevant for decision-making in a climate services context (Donat et al., 2023; Vaughan and Dessai, 2014; Delgado-Torres et al., 2025). The ResCorr isolates the added value of initialization beyond the historical simulations, providing insight into the role of internally generated variability. Together, these two metrics offer a more complete assessment of decadal prediction performance for energy-relevant indicators.

The predominantly positive PVpot trends over southern and central Europe are consistent with recent historical analyses. Segado-Moreno et al. (2026) have reported weak to positive RSDS trends over southern and central Europe when comparing observations from 1994–2004 and 2004–2023, in line with the patterns found here for the longer period 1961–2019. By contrast, studies focusing on future climate change suggest different responses, with projected decreases over northern Europe and weaker or near-neutral changes in the south (Jerez et al., 2015; Hou et al., 2021). Although these future-oriented results are not directly comparable to the present analysis, they provide context suggesting that the positive PVpot trends identified here over southern Europe are consistent with behaviours projected to strengthen in the future, whereas the future negative signals over northern Europe are not yet clearly expressed in the historical record.

### 4.2 Wind energy capacity factor (WCF)

Figure S9 shows the climatology (Figure S9a–e) and interannual standard deviation (Figure S9f–j) of WCF for the annual and seasonal means. The climatological patterns follow a distribution of wind resources over Europe, with higher WCF values over the North Atlantic and northern Europe and lower values over southern and Mediterranean regions, together with a clear seasonal cycle (Bett and Thornton, 2016) and higher values offshore than onshore. Unlike PVpot, WCF exhibits a non-negligible interannual standard deviation, with the largest values (up to 5–6 percentage points) occurring mainly in DJF and over northern Europe, reflecting stronger year-to-year wind variability. This reflects the intrinsically high variability of wind and the non-linear turbine power curve, which translates wind fluctuations into larger variations in WCF.

Figure 3a-e shows the ACC of WCF between DCPP and ERA5 for the annual mean and each season. Overall, the percentage of grid points with significant skill is generally low across Europe, with the highest values occurring in JJA (Figure 3d), followed by the annual mean (Figure 3a) and MAM (Figure 3c). Eastern Europe consistently exhibits higher skill, although the spatial patterns differ with season. In the annual mean and DJF (Figure 3a-b), there are some points with positive skill values over southern Iberia and southern France; the signal over southern France is weakly visible in MAM. In MAM, additionally,

https://doi.org/10.5194/egusphere-2026-1205
Preprint. Discussion started: 11 March 2026


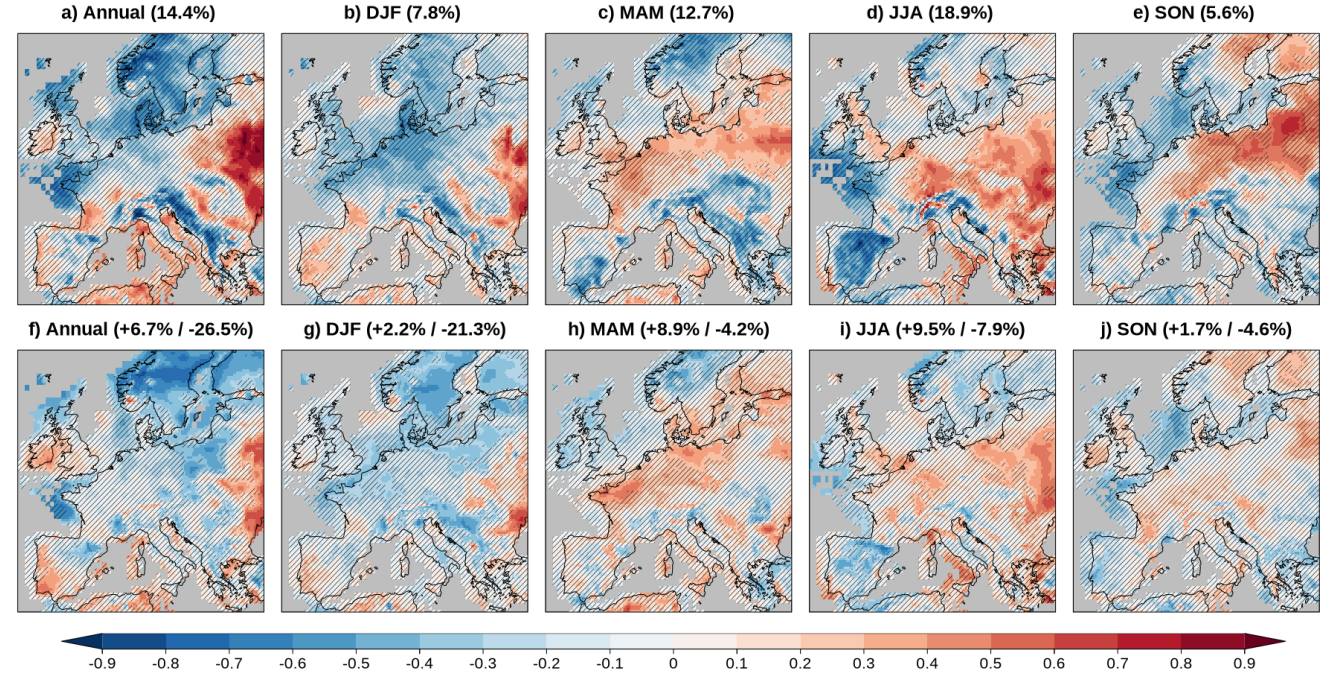


**Figure 3.** Same as Figure 1 but for WCF.

northern Germany and northern Poland show areas of significantly positive skill. In JJA, the high skill is present in many parts of central and eastern Europe and in points of the UK. In SON (Figure 3e), there are significant ACC values only in some points of Poland and the Baltics. Outside these regions, ACC values are generally low.

The spatial distribution and the percentage of significant grid points for WCF closely resemble those obtained for SFCWIND (Figure S5k-o), with only minor higher values for WCF. This similarity is expected as wind speed is the main driver of WCF.

Low predictive skill for wind-related variables is physically expected given the intrinsic characteristics of atmospheric circulation. Climate predictability partly depends on the nature and variability of the variable considered (Alizadeh, 2022). Variables that are strongly constrained by large-scale energy balances and evolve more slowly, such as TAS and RSDS, tend to be more predictable (Trenberth et al., 2009). In contrast, variables with higher variability and stronger dependence on regional and synoptic processes, such as SFCWIND or precipitation (PR), generally exhibit larger uncertainty (Gettelman and Rood, 2016; Slingo and Palmer, 2011). This behaviour is consistent with previous studies showing comparatively higher skill for decadal predictions for TAS than for PR (e.g. Smith et al., 2019; Delgado-Torres et al., 2022; Moreno-Montes et al., 2026).

Previous studies have examined the predictability of wind-related indicators for decadal predictions over Europe. Haas et al. (2015) and Moemken et al. (2016) have reported significant skill for regional peak winds and wind energy output (Eout) over central Europe, particularly for annual means and short lead times, using a statistical–dynamical downscaling approach applied to a single model. However, these results are not directly comparable to the present assessment of WCF, which relies on large-

https://doi.org/10.5194/egusphere-2026-1205
Preprint. Discussion started: 11 March 2026


scale model winds without regional downscaling and on a different wind-energy metric. More recently, Hutchins et al. (2025) have reported limited and spatially heterogeneous skill for surface wind over Europe, with significant predictability mainly confined to parts of central and eastern Europe, consistent with the patterns identified here.

The impact of model initialization on WCF skill is assessed using the ResCorr (Figure 3f–j). For all seasons and the annual mean, ResCorr exhibits both positive and negative values, indicating that initialization locally enhances skill in some regions while reducing it in others. For the annual mean and DJF (Figure 3f–g), initialization reduces WCF skill over Scandinavia and northern Europe, although HIST skill in these regions is already non-significant (Figure S10a–b), and in some parts of central Europe. The skill reduction may be related to the high interannual variability of WCF in these regions (Figure S9f–g), which can make the forecasts more sensitive to initialization errors. By contrast, initialization increases skill in the Atlantic coast of Iberia and Ireland for the annual mean, where HIST does not show significant skill, and over eastern Europe for the annual mean and DJF, where HIST does show it. In DJF, although ResCorr values are mostly non-significant over southern Europe, some regions with significantly positive HIST skill (Figure S10b) lose significance in the DCPP (Figure 3b), leading to a strong reduction in the overall percentage of significant area. In MAM (Figure 3h), positive ResCorr values are present in parts of northern France and Germany, and the DCPP (Figure 3c) has higher skill values than HIST (Figure S10h) over points of Germany but lower over points of the UK, resulting in a similar percentage of significant points. During JJA (Figure 3i), initialization increases skill over parts of eastern Europe and central Germany, while reducing it over Iberia, where HIST skill is already low (Figure S10d), resulting in a higher fraction of significant area for the DCPP than for the HIST. In SON (Figure 3j), ResCorr values remain close to zero and DCPP skill (Figure 3e) largely mirrors that of the HIST (Figure S10e). Overall, model initialization affects WCF skill mainly in winter and summer: it leads to a marked reduction of skill in DJF, while it enhances skill in JJA. In the remaining seasons, initialization has a limited impact and largely preserves the skill already present in the historical simulations.

Applying the same regionalization used for PVpot, regional trends of WCF differ markedly between ERA5 and the DCPP (Figure 4a–b). ERA5 shows no uniform behaviour, with both significantly positive and negative trends depending on region and season, whereas the DCPP exhibits predominantly significant negative trends across all regions and seasons. WCF trends follow similar patterns to those of SFCWIND (Figure S8e-f) for both ERA5 and the DCPP.

Consequently, regional correlations between ERA5 and the DCPP (Figure 4c) are significantly positive mainly where both datasets display coherent negative trends. This is most evident in Eastern Europe, with significant correlations for the annual mean, JJA and SON, and weaker agreement in DJF and MAM, consistent with the regions showing skill in Figure 3. Similar behaviour appears in Central Europe in JJA and SON, with additional agreement in Western Europe in MAM and weaker in Iberia in DJF. Elsewhere, differences in trend sign or magnitude lead to weak or negative correlations. Overall, these results emphasize the key role of trend consistency in explaining regional skill.

ResCorr regional values (Figure 4d) are generally non-significant, with a few isolated exceptions. A significantly positive ResCorr appears in Eastern Europe in JJA, aligned with the agreement in negative trends between ERA5 and the DCPP (Figure 4a–b) and the significantly positive correlation in Figure 4c. In addition, ResCorr is significantly positive in Central Europe in MAM, even though the correlation is not significant and trend agreement is weak, indicating the increase of skill due to

https://doi.org/10.5194/egusphere-2026-1205
Preprint. Discussion started: 11 March 2026


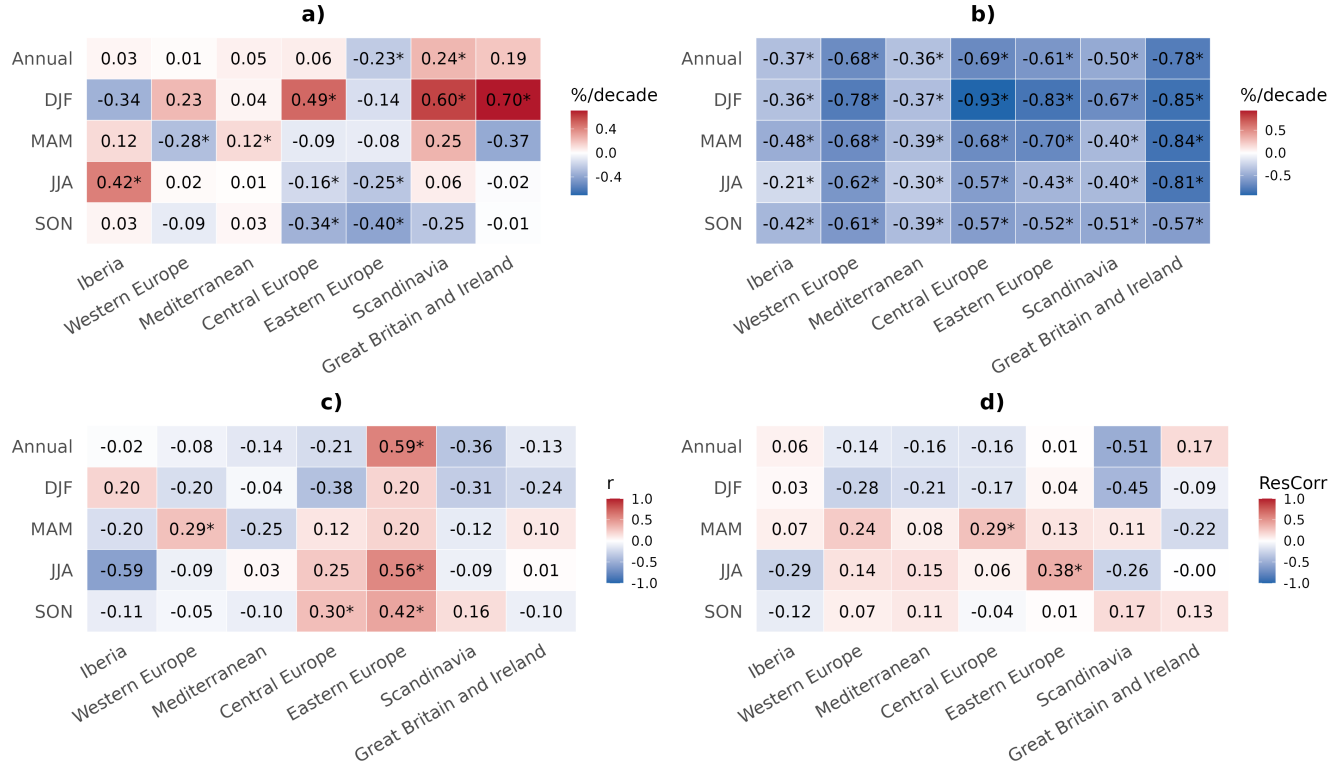


**Figure 4.** Same as Figure 2 but for WCF.

the initialization in this case. Other regions show non-significant but positive ResCorr values, suggesting local improvements due to initialization. In some of these cases, trends agree and correlations are positive (e.g. Western Europe in MAM). In others, trends have opposite signs and correlations are weak or negative, indicating that the limited skill comes mainly from initialization (e.g. Western Europe in JJA; Mediterranean in JJA and SON; Great Britain and Ireland in SON and annual). Conversely, there are regions where trends have the same sign and correlations are significantly positive, but ResCorr is close to zero (e.g. Eastern Europe in Annual and SON; Central Europe in JJA and SON). This suggests that most of the skill in those cases is explained by the externally forced trend rather than by initialization. Taken together, these results show that initialization can enhance skill in some regions, sometimes reinforcing existing trend agreement and in other cases providing additional skill independently of it.

The WCF trends found are consistent with signals reported in previous studies. Using climate projections, Pryor et al. (2005) have identified slight decreases in wind speed and wind energy density over northern Europe. Similarly, Olmo et al. (2026), analysing future climate scenarios, reported a projected weakening of near-surface winds over Europe, particularly towards the late 21st century. Although these projections are not directly comparable with the present analysis, they point to a tendency towards declining wind resources that may already be weakly emerging in current conditions. Observational analyses by Vautard et al. (2010) and Torralba et al. (2017a) have revealed spatially heterogeneous near-surface wind trends

https://doi.org/10.5194/egusphere-2026-1205
Preprint. Discussion started: 11 March 2026




across Europe, with predominantly negative signals in several regions. Together, these studies, based on different datasets and periods, indicate that declining wind signals have been reported in both modelling and observational contexts, while also highlighting the substantial uncertainty in the magnitude and spatial structure of historical wind changes.

### 4.3 Number of energy droughts (NED)

Figure S11 shows the climatology (Figure S11a–e) and interannual standard deviation (Figure S11f–j) of NED for the annual mean and each season. Overall, NED values are relatively high across Europe, reaching around 50% for the annual mean (Figure S11a). Seasonal patterns reflect the relative availability of each resource. In DJF and SON (Figure S11b,e), the NED values are generally high (between 40 and 100% in all the regions) and the highest ones occur particularly in mountainous regions (>80%), where low solar-Neff (<5%) (Figure S12b,e) and low wind-Neff (<10%) (Figure S12g,j) are found. Wind-Neff has values <10% in mountainous regions for all the seasons. In MAM (Figure S11c), higher NED values appear over parts of central Europe and some mountainous regions, mainly associated with low wind-Neff (Figure S12h), while solar-Neff (Figure S12c) decreases primarily with latitude. In JJA (Figure S11d), although being low (between 0 and 20%), higher NED values are largely confined to northern Europe, reflecting the strong latitudinal gradient in solar-Neff (Figure S12d), despite generally favourable solar conditions elsewhere. The standard deviation values are particularly high in DJF (Figure S11g) and over mountainous regions in JJA (Figure S11i). The high standard deviation observed over northern Poland and the Baltics in almost all seasons closely resembles the patterns found for the WCF standard deviation (Figure S8f–j), highlighting the strong influence of wind variability on NED.

The relatively high climatological values of the NED indicator mainly reflect the use of fixed, efficiency-based thresholds to define effective energy production. Previous studies have analyzed compound energy droughts using percentile-based metrics (e.g. Otero et al., 2022), which characterise relative extremes within each region. Despite these different definitions, the main seasonal patterns they report of higher drought frequencies in winter over southern Europe and in summer over northern regions are broadly consistent with our results. Here, fixed thresholds motivated by operational efficiency are adopted, an approach used in previous studies like Richardson et al. (2023). In our case, the prior calibration of all climate variables against ERA5 ensures consistent magnitudes, supporting the use of absolute, efficiency-related thresholds to assess compound energy droughts.

Figure 5a-e shows the ACC between the DCPP and ERA5 of NED. The highest fraction of significant ACC values occurs in JJA (Figure 5d), when most of eastern Europe and parts of central Europe and Iberia exhibit significant skill. The annual mean (Figure 5a) and MAM (Figure 5c) show significant ACC values over regions including parts of eastern Europe and the Atlantic coast of Iberia; however, MAM displays a slightly higher percentage of significant area, mainly due to additional significance over Italy. By contrast, skill is generally limited in DJF (Figure 5b), where significant ACC appears only in small areas of eastern Europe and Iberia, and in SON (Figure 5e), where skill is confined to parts of eastern Europe and the Baltics.

Figure S13 shows the ACC of the DCPP for solar-Neff (Figure S13a–e), wind-Neff (Figure S13f–j), and both-Neff (Figure S13k–o). The skill patterns of solar-Neff closely resemble those of solar PVpot (Figure 1a–e), while wind-Neff shows patterns similar to those of WCF (Figure 3a–e), as expected given that all three indicators reflect energy-production efficiency. By contrast, both-Neff exhibits more spatially fragmented skill, with isolated regions of significant values. In solar-Neff and both-

https://doi.org/10.5194/egusphere-2026-1205
Preprint. Discussion started: 11 March 2026


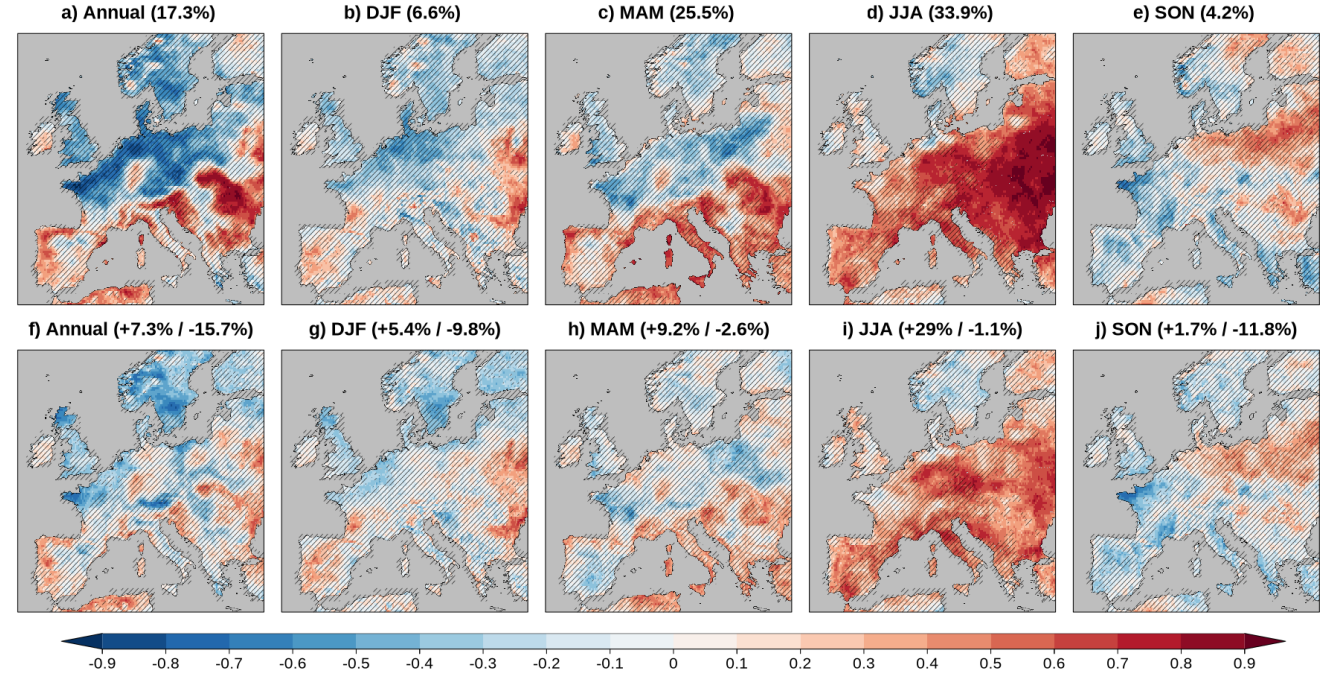


**Figure 5.** Same as Figure 1 but for NED.

Neff, some areas appear as missing values because correlations cannot be computed when the indicator remains equal to zero for all years, and solar energy droughts are expectable when the amount of daily sun hours is low (Figure S13b, e).

The spatial distribution of NED skill generally reflects the combined, but not necessarily simultaneous, contribution of solar- and wind-Neff predictability. For the annual mean (Figure 5a), significant NED skill over parts of eastern Europe and Iberia coincides with regions where both solar-Neff (Figure S13a) and wind-Neff (Figure S13f) are skillful. By contrast, over parts of the Alps and southeastern region, NED exhibits significant skill despite wind-Neff being non-significant, indicating a dominant contribution from solar-Neff. In DJF (Figure 5b), NED skill over Iberia and eastern Europe aligns mainly with wind-Neff skill (Figure S13g). In MAM (Figure 5c), NED skill over southern and southeastern Europe follows the solar-Neff signal, although NED remains non-significant in many regions where solar-Neff shows skill. In JJA (Figure 5d), the widespread NED skill closely follows the solar-Neff pattern (Figure S13d), only showing lower values over parts of Western Europe. Finally, in SON (Figure 5e), NED skill is confined to parts of Poland and the Baltic region, closely matching the wind-Neff skill pattern (Figure S13j) and in points of southeastern Europe, which are skillful at solar-Neff (Figure S13e).

Overall, these results may indicate that NED predictability is strongly seasonally modulated by the dominant energy source. During periods of high solar availability (JJA and, in the southern region, MAM), NED skill is largely driven by solar-Neff, whereas in low-radiation seasons (DJF and SON) wind-Neff becomes the main modulator.

https://doi.org/10.5194/egusphere-2026-1205
Preprint. Discussion started: 11 March 2026


The heterogeneous ResCorr patterns (Figure 5f–j), with both positive and negative values in all seasons, indicate that the impact of initialization on this indicator varies across seasons and regions. In the annual mean (Figure 5f), positive ResCorr values appear along the Atlantic coast of Iberia and in parts of eastern Europe, while negative values dominate along the rest of the Atlantic coast. Although the DCPP skill pattern (Figure 5a) resembles that of the HIST (Figure S14a) and ResCorr is not significant there, the skill of DCPP is lower than that of HIST in eastern Iberia and over a large part of Italy, as well as in the fraction of significant grid points. In DJF (Figure 5g), ResCorr is positive in parts of eastern and Southwestern Europe but negative in parts of northern Europe, resulting in a lower skill for DCPP (Figure 5b) than for HIST (Figure S14b). In MAM (Figure 5h), initialization enhances skill over parts of southern and eastern Europe while reducing it over Iberia, leading to a modest improvement of DCPP skill relative to HIST (Figure 5c vs Figure S14c). During JJA (Figure 5i), positive ResCorr values extend across large areas of central and southern Europe, and DCPP shows clearly higher skill than HIST (Figure 5d vs Figure S14d). By contrast, in SON (Figure 5j), ResCorr is predominantly negative with only isolated positive values, resulting in a lower fraction of significant skill in DCPP (Figure 5e) compared to HIST (Figure S14e). For this indicator, initialization generally increases predictability under conditions of higher sunshine duration (JJA and MAM) and reduces it under the opposite conditions (DJF and SON).

Figure 6 shows the regional trends of NED for ERA5 (a), for the DCPP (b), the corresponding correlations (c), and the ResCorr (d) across the seven sub-regions defined above. In some regions and seasons, ERA5 and DCPP exhibit similar trends, while in others they show opposite signs. In JJA, Iberia, Western Europe, Mediterranean, Central and Eastern Europe display significant negative trends in both datasets, which results in significantly positive correlations (Figure 6c). A similar behaviour is found for the annual mean and MAM in Iberia, Western Europe and Mediterranean. In addition, there are cases where both ERA5 and DCPP show significantly positive trends, leading to positive, though non-significant, correlations, such as in DJF for Iberia, in SON for Central Europe, and in DJF and SON for Eastern Europe. In the remaining regions and seasons, ERA5 and DCPP trends generally differ in sign, typically negative in ERA5 and positive in the DCPP, resulting in correlations that are weak or negative. Overall, these results again underline the importance of consistently reproducing the trend for obtaining high correlation values.

ResCorr (Figure 6d) partly mirrors the correlation patterns shown in Figure 6c. Regions and seasons with significantly positive ResCorr values (notably Iberia, Mediterranean, Central and Eastern Europe in JJA; and more weakly Iberia in DJF, Mediterranean in MAM, and Eastern Europe in SON) correspond to cases where correlations are also significantly positive. This indicates that, in these cases, initialization enhances skill beyond the externally forced signal already contributing to the correlation. However, there are also cases with significantly positive correlations but low or negative ResCorr values (e.g. Iberia in MAM and Annual; Mediterranean in Annual). In these situations, the agreement in trends between ERA5 and the DCPP explains most of the skill, while initialization adds little or even decreases predictive value.

NED variability is largely controlled by the energy source that dominates effective production in each season: wind in DJF and SON, and solar in JJA and, secondarily, in MAM. As a result, NED trends in DJF and SON tend to be anticorrelated with WCF trends (Figure 4). In the DCPP, WCF trends are consistently negative across regions, while NED trends are generally positive, leading to opposite signs. In ERA5, WCF trends are more heterogeneous, and this spatial variability is reflected in the

https://doi.org/10.5194/egusphere-2026-1205
Preprint. Discussion started: 11 March 2026


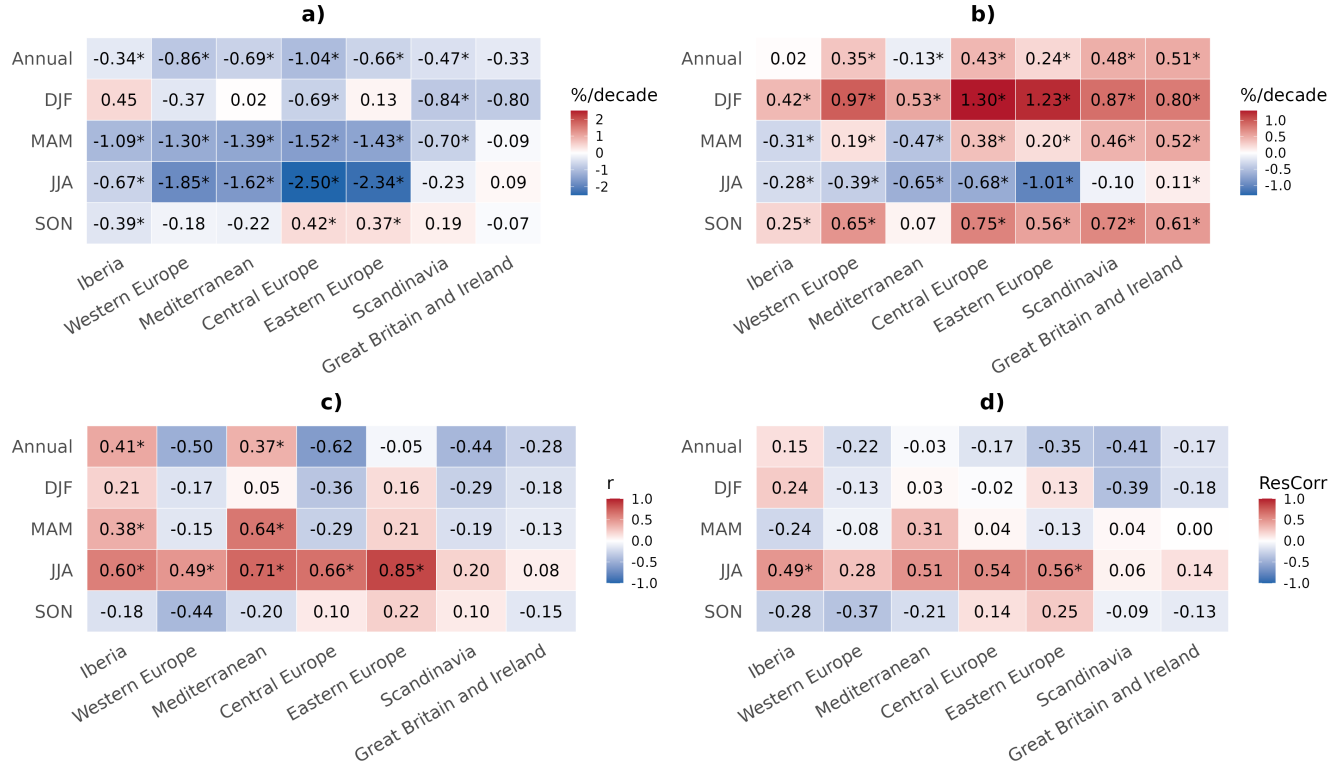


**Figure 6.** Same as Figure 2 but for NED.

NED trends; for example, positive WCF trends in DJF over Scandinavia and Great Britain and Ireland and negative trends over Iberia correspond to opposite-sign trends in NED. A similar, though weaker, relationship is found between NED and PVpot in JJA and in southern regions during MAM. In these cases, positive trends in PVpot (Figure 2) for both ERA5 and the DCPP are associated with generally negative NED trends, particularly in JJA and in southern regions during MAM. This link is clearer in ERA5 and less pronounced in DCPP.

The negative NED trends identified in ERA5 for the recent past are consistent with the ERA5-based analysis of (Meng et al., 2025), which have reported a decrease in the frequency of renewable energy droughts under present-day conditions, despite differences in indicator definition. Additionally, DCPP trends show seasonal patterns that broadly resemble the future evolution of hybrid energy droughts projected by (Kapica et al., 2024), particularly in DJF and SON. Although their results refer to future climate scenarios and are based on a different definition of compound events, the similarities suggest that some of the changes projected for the future may already be emerging in the decadal predictions analyzed here.

https://doi.org/10.5194/egusphere-2026-1205
Preprint. Discussion started: 11 March 2026


## 5 Conclusions

The renewable energy sector is strongly influenced by variability and long-term changes in key climate variables such as temperature, solar radiation and wind speed. However, the intermediate timescale of the coming years remains comparatively underexplored, and there is a clear need for tailored climate information to bridge the gap between decadal prediction advances and their application in renewable energy planning.

This study evaluates the predictive skill of a multi-model of decadal predictions (DCPP) for energy-relevant indicators over Europe, focusing on photovoltaic potential (PVpot), wind capacity factor (WCF), and the compound indicator number of energy droughts (NED) for forecast years 1–3. Skill is assessed using the ACC between the DCPP and ERA5, and the impact of model initialization is estimated with the ResCorr relative to historical simulations. In addition to grid-point analyses, sub-regional mean trends and correlations are examined to explore the relationship between long-term changes and predictive skill.

PVpot shows the highest and most spatially coherent skill among the indicators analyzed. Skill is significantly positive over large parts of the region at the annual scale and during MAM and JJA, while it is weaker and more spatially limited in DJF and SON. This strong seasonal dependence indicates that PVpot predictability is highest during periods of higher and persistent solar radiation, while such predictability is more limited under weaker and more variable radiative conditions. The spatial and seasonal patterns of PVpot skill closely follow those of surface downwelling shortwave radiation (RSDS), its main driver. PVpot skill is slightly lower than RSDS skill because the indicator is also modulated by near-surface air temperature (TAS) and surface wind speed (SFCWIND), which act as secondary constraints on predictability.

Initialization clearly improves skill in the annual mean and in JJA, mainly by enhancing already positive skill values of the multi-model of historical simulations (HIST). In DJF and SON, the added value of initialization is limited and spatially heterogeneous, with localized improvements and degradations. Overall, initialization tends to amplify existing PVpot predictability in HIST.

WCF exhibits lower and more spatially heterogeneous skill than PVpot, reflecting the higher intrinsic variability of wind and its strong sensitivity to synoptic-scale circulation. Significant skill is consistently found over parts of eastern Europe across seasons, while other regions show skill only seasonally: central Europe in JJA, southern Europe in DJF, and northern Europe in MAM and SON. The spatial distribution of WCF skill closely mirrors that of SFCWIND, confirming wind variability as the primary control on WCF predictability.

Initialization tends to enhance skill in summer and reduce it in winter, while its impact is generally small in the transition seasons. As for PVpot, initialization mainly improves skill where historical simulations already show some skill. The overall low skill for WCF is partly associated with opposite trend signs between ERA5 and the DCPP in many regions and seasons.

The compound indicator NED displays predictability characteristics that reflect the combined influence of solar and wind resources. NED skill is highest in JJA, followed by the annual mean and MAM, and is generally limited in DJF and SON. NED predictability does not require simultaneous skill in both components: in some regions it emerges where both solar-Neff and wind-Neff are predictable, while in others it is dominated by a single source. This highlights the non-linear nature of compound energy droughts and the importance of interactions between resources.

https://doi.org/10.5194/egusphere-2026-1205
Preprint. Discussion started: 11 March 2026


Seasonal differences in NED skill reflect the dominant energy source. During high-radiation periods (JJA and partly MAM), NED predictability is mainly driven by solar-Neff, whereas during low-radiation seasons (DJF and SON) wind-Neff becomes the main contributor. The impact of initialization on NED follows this seasonal dependence, enhancing skill when the dominant source is more predictable and reducing it otherwise. These results show that energy-relevant indicators derived from decadal predictions can provide actionable information to anticipate energy droughts. However, predictability is strongly dependent on season, region and indicator. Initialization generally enhances skill where some degree of predictability already exists but rarely creates new skill when historical simulations do not have it.

By evaluating compound energy indicators, explicitly separating total skill from the added value of initialization, and analysing results at the regional scale, this study advances beyond variable-based assessments and provides a more application-oriented understanding of decadal predictability for renewable energy. These findings highlight both the potential and the limitations of decadal predictions for energy-related applications and underscore the need to clearly communicate where and when such information is reliable.

Several limitations should be noted. ERA5 is the only reference dataset used, and reanalysis uncertainties, especially for wind, may affect skill estimates. However, ERA5 has been identified as the best reanalysis for wind (Ramon et al., 2019) and Global Wind Atlas has been used to correct it for a more accurate representation. Secondly, fixed, efficiency-based thresholds, although operationally motivated, may limit sensitivity and transferability across regions or technologies. Besides, temporal aggregation choices influence the indicators, particularly for wind, given the finer temporal resolution of turbine power curves. In addition, the power-law extrapolation used to estimate 100 m wind speeds assumes neutral stability and may be less representative under non-neutral atmospheric conditions, which could affect the reliability of local-scale decadal predictions. Finally, the ACC and ResCorr metrics capture correlation-based skill but do not fully describe other aspects relevant for operational decision-making, such as reliability or the representation of extreme events. Other metrics might be selected depending on the climate forecast products required by the energy users.

Future work could assess how sensitive the indicators are to the choice of thresholds (e.g. different RSDS or WCF limits), compare results using alternative reanalyses or observation-based datasets. The framework could also be extended to include electricity demand, which would allow a more comprehensive assessment of supply–demand imbalances and increase the relevance of the indicators for system operators and energy planners. In addition, hybrid approaches that combine percentile-based metrics with physically motivated thresholds may help balance climatological comparability and operational relevance when assessing compound renewable-energy risks.

*Code availability.* We acknowledge the use of the startR, s2dv, CSTools, multiApply, and CSIndicators R-language-based software packages, all of them available on the Comprehensive R Archive Network (CRAN; https://cran.r-project.org/, last access: 2 March 2026). The code used during the study is available from the corresponding author on reasonable request.

https://doi.org/10.5194/egusphere-2026-1205
Preprint. Discussion started: 11 March 2026


*Data availability.* All datasets used in the study are publicly available. SEAS5 predictions and ERA5 reanalysis data are available from the Copernicus Climate Data Store (CDS; https://cds.climate.copernicus.eu/, last access: 2 March 2026). The decadal predictions, historical simulations and climate projections are available on the Earth System Grid Federation system (ESGF; https://esgf.github.io/, last access: 2 March 2026).

*Author contributions.* SMM and CDT designed the study. SMM carried out the analysis and wrote the first draft. All authors contributed equally to the interpretation of results and writing thereafter.

*Competing interests.* The contact author has declared that none of the authors has any competing interests.

*Acknowledgements.* This study has been supported by the Spanish national project BOREAS (PID2022-140673OA-I00) funded by MICIU/AEI/10.13039/501100011033 and by ERDF, EU. SMM gratefully acknowledges financial support from the Spanish Ministry for Science and Innovation (FPI PREP2022-000684, funded by MCIN/AEI/10.13039/501100011033). MEO is funded by the AI4Science PN070500 fellowship within the "Generación D" initiative, Red.es, Ministerio para la Transformación Digital y de la Función Pública, for talent attraction (C005/24-ED CV1). Funded by the European Union NextGenerationEU funds, through PRTR. VT has received funding from the EU Horizon 2020 Marie Skłodowska-Curie grant 101152499 (SINFONIA).

https://doi.org/10.5194/egusphere-2026-1205
Preprint. Discussion started: 11 March 2026


## References

Agency, E. E.: Share of energy consumption from renewable sources in Europe, Published: 26.10. 022, 2022.

Alizadeh, O.: Advances and challenges in climate modeling, Climatic Change, 170, 18, 2022.

Aranyossy, A., De Luca, P., Delgado-Torres, C., Solaraju-Murali, B., Samso Cabre, M., and Donat, M. G.: Multi-annual predictions of hot, dry and hot-dry compound extremes, Earth System Dynamics, 16, 2225–2251, 2025.

Association, W. M. et al.: WMO global annual to decadal climate update, 2023.

Bellucci, A., Haarsma, R., Gualdi, S., Athanasiadis, P., Caian, M., Cassou, C., Fernandez, E., Germe, A., Jungclaus, J., Kröger, J., et al.: An assessment of a multi-model ensemble of decadal climate predictions, Climate Dynamics, 44, 2787–2806, 2015.

Bett, P. E. and Thornton, H. E.: The climatological relationships between wind and solar energy supply in Britain, Renewable Energy, 87, 96–110, 2016.

Bett, P. E., Thornton, H. E., Troccoli, A., De Felice, M., Suckling, E., Dubus, L., Saint-Drenan, Y.-M., and Brayshaw, D. J.: A simplified seasonal forecasting strategy, applied to wind and solar power in Europe, Climate services, 27, 100 318, 2022.

Bloomfield, H. C., Brayshaw, D. J., Gonzalez, P. L., and Charlton-Perez, A.: Sub-seasonal forecasts of demand and wind power and solar power generation for 28 European countries, Earth System Science Data, 13, 2259–2274, 2021.

Boccard, N.: Capacity factor of wind power realized values vs. estimates, energy policy, 37, 2679–2688, 2009.

Boer, G. J., Smith, D. M., Cassou, C., Doblas-Reyes, F., Danabasoglu, G., Kirtman, B., Kushnir, Y., Kimoto, M., Meehl, G. A., Msadek, R., et al.: The decadal climate prediction project (DCPP) contribution to CMIP6, Geoscientific Model Development, 9, 3751–3777, 2016.

Brower, M.: Wind resource assessment: a practical guide to developing a wind project, John Wiley & Sons, 2012.

Carvalho, D., Rocha, A., Costoya, X., DeCastro, M., and Gómez-Gesteira, M.: Wind energy resource over Europe under CMIP6 future climate projections: What changes from CMIP5 to CMIP6, Renewable and Sustainable Energy Reviews, 151, 111 594, 2021.

Castillo, C. P., e Silva, F. B., and Lavalle, C.: An assessment of the regional potential for solar power generation in EU-28, Energy policy, 88, 86–99, 2016.

Challinor, A. J., Adger, W. N., and Benton, T. G.: Climate risks across borders and scales, Nature Climate Change, 7, 621–623, 2017.

Chenni, R., Makhlouf, M., Kerbache, T., and Bouzid, A.: A detailed modeling method for photovoltaic cells, Energy, 32, 1724–1730, 2007.

Cionni, I., Lledo, L., Torralba, V., and Dell'Aquila, A.: Seasonal predictions of energy-relevant climate variables through Euro-Atlantic Teleconnections, Climate Services, 26, 100 294, 2022.

Clark, R. T., Bett, P. E., Thornton, H. E., and Scaife, A. A.: Skilful seasonal predictions for the European energy industry, Environmental Research Letters, 12, 024 002, 2017.

Commission, E.: Powering a climate-neutral economy: An EU strategy for energy system integration, 2020.

Corti, S., Weisheimer, A., Palmer, T., Doblas-Reyes, F., and Magnusson, L.: Reliability of decadal predictions, Geophysical Research Letters, 39, 2012.

Delgado-Torres, C., Donat, M. G., Gonzalez-Reviriego, N., Caron, L.-P., Athanasiadis, P. J., Bretonnière, P.-A., Dunstone, N. J., Ho, A.-C., Nicoli, D., Pankatz, K., et al.: Multi-model forecast quality assessment of CMIP6 decadal predictions, Journal of Climate, 35, 4363–4382, 2022.

Delgado-Torres, C., Donat, M. G., Soret, A., González-Reviriego, N., Bretonnière, P.-A., Ho, A.-C., Pérez-Zanón, N., Samso Cabre, M., and Doblas-Reyes, F. J.: Multi-annual predictions of the frequency and intensity of daily temperature and precipitation extremes, Environmental Research Letters, 18, 034 031, 2023.

https://doi.org/10.5194/egusphere-2026-1205
Preprint. Discussion started: 11 March 2026


Delgado-Torres, C., Octenjak, S., Marcos-Matamoros, R., Pérez-Zanón, N., Baulenas, E., Doblas-Reyes, F. J., Donat, M. G., Lwiza, L. M., Milders, N., Soret, A., et al.: Supporting food security with multi-annual climate information: Co-production of climate services for the Southern African Development Community, Science of The Total Environment, 975, 179 259, 2025.

Donat, M. G., Delgado-Torres, C., De Luca, P., Mahmood, R., Ortega, P., and Doblas-Reyes, F. J.: How credibly do CMIP6 simulations capture historical mean and extreme precipitation changes?, Geophysical Research Letters, 50, e2022GL102 466, 2023.

Done, J. M., Morss, R. E., Lazrus, H., Towler, E., Tye, M. R., Ge, M., Das, T., Munévar, A., Hewitt, J., and Hoeting, J. A.: Toward usable predictive climate information at decadal timescales, One Earth, 4, 1297–1309, 2021.

Duffie, J. A. and Beckman, W. A.: Solar engineering of thermal processes, Wiley New York, 1980.

Dunstone, N., Lockwood, J., Solaraju-Murali, B., Reinhardt, K., Tsartsali, E. E., Athanasiadis, P. J., Bellucci, A., Brookshaw, A., Caron, L.-P., Doblas-Reyes, F. J., et al.: Towards useful decadal climate services, Bulletin of the American Meteorological Society, 103, E1705–E1719, 2022.

Elsner, J. B. and Schmertmann, C.: Assessing forecast skill through cross validation, Weather and Forecasting, 9, 619–624, 1994.

Ely, C. R., Brayshaw, D. J., Methven, J., Cox, J., and Pearce, O.: Implications of the North Atlantic Oscillation for a UK–Norway renewable power system, Energy Policy, 62, 1420–1427, 2013.

Eyring, V., Bony, S., Meehl, G. A., Senior, C. A., Stevens, B., Stouffer, R. J., and Taylor, K. E.: Overview of the Coupled Model Intercomparison Project Phase 6 (CMIP6) experimental design and organization, Geoscientific Model Development, 9, 1937–1958, 2016.

Gettelman, A. and Rood, R. B.: Demystifying climate models: A users guide to earth system models, Springer, 2016.

Ghosh, S., Dey, S., Ganguly, D., Baidya Roy, S., and Bali, K.: Cleaner air would enhance India's annual solar energy production by 6–28 TWh, Environmental Research Letters, 17, 054 007, 2022.

Ghosh, S., Ganguly, D., Dey, S., and Chowdhury, S. G.: Future photovoltaic potential in India: navigating the interplay between air pollution control and climate change mitigation, Environmental Research Letters, 19, 124 030, 2024.

Gonzalez, P. L., Brayshaw, D. J., and Zappa, G.: The contribution of North Atlantic atmospheric circulation shifts to future wind speed projections for wind power over Europe, Climate Dynamics, 53, 4095–4113, 2019.

Haas, R., Reyers, M., and Pinto, J. G.: Decadal predictability of regional-scale peak winds over Europe using the Earth System Model of the Max-Planck-Institute for Meteorology, Meteorol. Z, 25, 739–752, 2015.

Heide, D., Von Bremen, L., Greiner, M., Hoffmann, C., Speckmann, M., and Bofinger, S.: Seasonal optimal mix of wind and solar power in a future, highly renewable Europe, Renewable Energy, 35, 2483–2489, 2010.

Hersbach, H., Bell, B., Berrisford, P., Hirahara, S., Horányi, A., Muñoz-Sabater, J., Nicolas, J., Peubey, C., Radu, R., Schepers, D., et al.: The ERA5 global reanalysis, quarterly journal of the royal meteorological society, Quarterly Journal of the Royal Meteorological Society, 2020.

Hou, X., Wild, M., Folini, D., Kazadzis, S., and Wohland, J.: Climate change impacts on solar power generation and its spatial variability in Europe based on CMIP6, Earth System Dynamics, 12, 1099–1113, 2021.

Hutchins, B. W., Brayshaw, D. J., Shaffrey, L. C., Thornton, H. E., and Smith, D. M.: Decadal prediction for the European energy sector, Meteorological Applications, 32, e70 054, 2025.

IEA: Renewables 2023, 2024.

IEC, I.: 61400-1: Wind turbines part 1: Design requirements, International Electrotechnical Commission, 177, 2005.

Jerez, S., Tobin, I., Vautard, R., Montávez, J. P., López-Romero, J. M., Thais, F., Bartok, B., Christensen, O. B., Colette, A., Déqué, M., et al.: The impact of climate change on photovoltaic power generation in Europe, Nature communications, 6, 10 014, 2015.

https://doi.org/10.5194/egusphere-2026-1205
Preprint. Discussion started: 11 March 2026


Jerez, S., Tobin, I., Turco, M., Jiménez-Guerrero, P., Vautard, R., and Montávez, J. P.: Future changes, or lack thereof, in the temporal variability of the combined wind-plus-solar power production in Europe, Renewable energy, 139, 251–260, 2019.

Kalverla, P. C., Duncan Jr, J. B., Steeneveld, G.-J., and Holtslag, A. A.: Low-level jets over the North Sea based on ERA5 and observations: together they do better, Wind Energy Science, 4, 193–209, 2019.

Kapica, J., Jurasz, J., Canales, F. A., Bloomfield, H., Guezgouz, M., De Felice, M., and Kobus, Z.: The potential impact of climate change on European renewable energy droughts, Renewable and Sustainable Energy Reviews, 189, 114 011, 2024.

Kealy, T., Barrett, M., and Kearney, D.: How profitable are wind turbine projects? An empirical analysis of a 3.5 MW wind farm in Ireland, International journal on recent technologies in mechanical and electrical engineering, 2015.

Kharin, V., Boer, G., Merryfield, W., Scinocca, J., and Lee, W.-S.: Statistical adjustment of decadal predictions in a changing climate, Geophysical Research Letters, 39, 2012.

Lledó, L., Ramon, J., Soret, A., and Doblas-Reyes, F.-J.: Seasonal prediction of renewable energy generation in Europe based on four teleconnection indices, Renewable Energy, 186, 420–430, 2022.

MacLeod, D., Torralba, V., Davis, M., and Doblas-Reyes, F.: Transforming climate model output to forecasts of wind power production: how much resolution is enough?, Meteorological Applications, 25, 1–10, 2018.

Mavromatakis, F., Makrides, G., Georghiou, G., Pothrakis, A., Franghiadakis, Y., Drakakis, E., and Koudoumas, E.: Modeling the photovoltaic potential of a site, Renewable energy, 35, 1387–1390, 2010.

Meehl, G. A., Goddard, L., Murphy, J., Stouffer, R. J., Boer, G., Danabasoglu, G., Dixon, K., Giorgetta, M. A., Greene, A. M., Hawkins, E., et al.: Decadal prediction: can it be skillful?, Bulletin of the American Meteorological Society, 90, 1467–1486, 2009.

Meng, Y., Schmidt, J., Zscheischler, J., and Bevacqua, E.: Climate-driven compounding effects and historical trends in renewable electricity droughts in Europe, Applied Energy, 401, 126 623, 2025.

Moemken, J., Reyers, M., Buldmann, B., and Pinto, J. G.: Decadal predictability of regional scale wind speed and wind energy potentials over Central Europe, Tellus A: Dynamic Meteorology and Oceanography, 68, 29 199, 2016.

Monforti, F., Huld, T., Bódis, K., Vitali, L., D'isidoro, M., and Lacal-Arántegui, R.: Assessing complementarity of wind and solar resources for energy production in Italy. A Monte Carlo approach, Renewable Energy, 63, 576–586, 2014.

Moreno-Montes, S., Delgado-Torres, C., Duzenli, E., Pérez-Zanón, N., Marcos-Matamoros, R., and Soret, A.: Comparative analysis of statistical downscaling methods for multi-model decadal climate predictions over Western Europe, Climate Services, 42, 100 639, https://doi.org/https://doi.org/10.1016/j.cliser.2026.100639, 2026.

Müller, J., Folini, D., Wild, M., and Pfenninger, S.: CMIP-5 models project photovoltaics are a no-regrets investment in Europe irrespective of climate change, Energy, 171, 135–148, 2019.

Olmo, M., Moreno-Montes, S., Trascasa-Castro, P., Balmaceda-Huarte, R., Delgado-Torres, C., Torralba, V., and Soret, A.: Disentangling the spread in wind projections over Europe and the impacts on energy generation., Earth's future, under review, 2026.

O'Neill, B. C., Tebaldi, C., Van Vuuren, D. P., Eyring, V., Friedlingstein, P., Hurtt, G., Knutti, R., Kriegler, E., Lamarque, J.-F., Lowe, J., et al.: The scenario model intercomparison project (ScenarioMIP) for CMIP6, Geoscientific Model Development, 9, 3461–3482, 2016.

Otero, N., Martius, O., Allen, S., Bloomfield, H., and Schaefli, B.: A copula-based assessment of renewable energy droughts across Europe, Renewable Energy, 201, 667–677, 2022.

Panofsky, H. A. and Brier, G. W.: Some applications of statistics to meteorology, Mineral Industries Extension Services, College of Mineral Industries . . . , 1958.

https://doi.org/10.5194/egusphere-2026-1205
Preprint. Discussion started: 11 March 2026


Paxian, A., Reinhardt, K., Pankatz, K., Pasternack, A., Lorza-Villegas, M. P., Scheibel, M., Hoff, A., Mannig, B., Lorenz, P., and Früh, B.: High-resolution decadal drought predictions for German water boards: a case study for the Wupper catchment, Frontiers in Climate, 4, 867 814, 2022.

Payne, M. R., Danabasoglu, G., Keenlyside, N., Matei, D., Miesner, A. K., Yang, S., and Yeager, S. G.: Skilful decadal-scale prediction of fish habitat and distribution shifts, Nature Communications, 13, 2660, 2022.

Pérez-Zanón, N., Ho, A.-C., Chou, C., Lledó, L., Marcos-Matamoros, R., Rifà, E., and González-Reviriego, N.: CSIndicators: Get tailored climate indicators for applications in your sector, 2023.

Priestley, M. D., Stephenson, D. B., Scaife, A. A., Bannister, D., Allen, C. J., and Wilkie, D.: Forced trends and internal variability in climate change projections of extreme European windstorm frequency and severity, Quarterly Journal of the Royal Meteorological Society, 150, 4933–4950, 2024.

Pryor, S., Schoof, J., and Barthelmie, R.: Climate change impacts on wind speeds and wind energy density in northern Europe: empirical downscaling of multiple AOGCMs, Climate Research, 29, 183–198, 2005.

Radziemska, E.: The effect of temperature on the power drop in crystalline silicon solar cells, Renewable energy, 28, 1–12, 2003.

Ramon, J., Lledó, L., Torralba, V., Soret, A., and Doblas-Reyes, F. J.: What global reanalysis best represents near-surface winds?, Quarterly Journal of the Royal Meteorological Society, 145, 3236–3251, 2019.

Ramon, J., Lledó, L., Ferro, C. A., and Doblas-Reyes, F. J.: Uncertainties in the observational reference: Implications in skill assessment and model ranking of seasonal predictions, Quarterly Journal of the Royal Meteorological Society, 150, 897–910, 2024.

Richardson, D., Pitman, A., and Ridder, N.: Climate influence on compound solar and wind droughts in Australia, npj Climate and Atmospheric Science, 6, 184, 2023.

Segado-Moreno, L. C., Ruiz-Arias, J. A., Montávez, J. P., and Betak, J.: Past, current and future solar radiation trends in Europe: Multi-source assessment of the role of clouds and aerosols, Remote Sensing of Environment, 333, 115 122, 2026.

Slingo, J. and Palmer, T.: Uncertainty in weather and climate prediction, Philosophical Transactions of the Royal Society A: Mathematical, Physical and Engineering Sciences, 369, 4751–4767, 2011.

Smith, D., Eade, R., Scaife, A., Caron, L.-P., Danabasoglu, G., DelSole, T., Delworth, T., Doblas-Reyes, F., Dunstone, N., Hermanson, L., et al.: Robust skill of decadal climate predictions, Npj Climate and Atmospheric Science, 2, 13, 2019.

Smith, D. M., Scaife, A. A., and Kirtman, B. P.: What is the current state of scientific knowledge with regard to seasonal and decadal forecasting?, Environmental Research Letters, 7, 015 602, 2012.

Solaraju-Murali, B., Bojovic, D., Gonzalez-Reviriego, N., Nicodemou, A., Terrado, M., Caron, L.-P., and Doblas-Reyes, F. J.: How decadal predictions entered the climate services arena: an example from the agriculture sector, Climate services, 27, 100 303, 2022.

Solomon, S.: Climate change 2007-the physical science basis: Working group I contribution to the fourth assessment report of the IPCC, vol. 4, Cambridge university press, 2007.

Soret, A., Gonzalez, P., Bloomfield, H., Masato, G., Goutham, N., Plougonven, R., and Torralba, V.: Subseasonal-to-seasonal climate predictions for energy, in: Sub-seasonal to Seasonal Prediction, pp. 779–807, Elsevier, 2026.

Storch, H. v. and Zwiers, F. W.: Statistical Analysis in Climate Research, Cambridge University Press, 1999.

Suckling, E. B., van Oldenborgh, G. J., Eden, J. M., and Hawkins, E.: An empirical model for probabilistic decadal prediction: global attribution and regional hindcasts, Climate Dynamics, 48, 3115–3138, 2017.

Šúri, M., Huld, T. A., Dunlop, E. D., and Ossenbrink, H. A.: Potential of solar electricity generation in the European Union member states and candidate countries, Solar energy, 81, 1295–1305, 2007.

https://doi.org/10.5194/egusphere-2026-1205
Preprint. Discussion started: 11 March 2026


Torralba, V., Doblas-Reyes, F. J., and Gonzalez-Reviriego, N.: Uncertainty in recent near-surface wind speed trends: a global reanalysis intercomparison, Environmental Research Letters, 12, 114 019, 2017a.

Torralba, V., Doblas-Reyes, F. J., MacLeod, D., Christel, I., and Davis, M.: Seasonal climate prediction: a new source of information for the management of wind energy resources, Journal of Applied Meteorology and Climatology, 56, 1231–1247, 2017b.

Touma, J. S.: Dependence of the wind profile power law on stability for various locations, Journal of the Air Pollution Control Association, 27, 863–866, 1977.

Trenberth, K. E., Fasullo, J. T., and Kiehl, J.: Earth's global energy budget, Bulletin of the american meteorological society, 90, 311–324, 2009.

Tsartsali, E., Athanasiadis, P., Materia, S., Bellucci, A., Nicolì, D., and Gualdi, S.: Predicting precipitation on the decadal timescale: A prototype climate service for the hydropower sector, Climate Services, 32, 100 422, 2023.

van Oldenborgh, G. J., Doblas-Reyes, F. J., Wouters, B., and Hazeleger, W.: Decadal prediction skill in a multi-model ensemble, Climate dynamics, 38, 1263–1280, 2012.

Vaughan, C. and Dessai, S.: Climate services for society: origins, institutional arrangements, and design elements for an evaluation framework, Wiley Interdisciplinary Reviews: Climate Change, 5, 587–603, 2014.

Vautard, R., Cattiaux, J., Yiou, P., Thépaut, J.-N., and Ciais, P.: Northern Hemisphere atmospheric stilling partly attributed to an increase in surface roughness, Nature geoscience, 3, 756–761, 2010.

Weide Luiz, E. and Fiedler, S.: Spatiotemporal observations of nocturnal low-level jets and impacts on wind power production, Wind Energy Science, 7, 1575–1591, 2022.

Wilks, D. S.: Forecast verification, in: International geophysics, vol. 100, pp. 301–394, Elsevier, 2011.

Wiser, R., Bolinger, M., Hoen, B., Millstein, D., Rand, J., Barbose, G., Darghouth, N., Gorman, W., Jeong, S., O'Shaughnessy, E., et al.: Land-based wind market report: 2023 edition, Tellus A: Dynamic Meteorology and Oceanography, 2023.

World Meteorological Organization: WMO Global Annual to Decadal Climate Update, 2024–2028, Tech. rep., World Meteorological Organization, Geneva, Switzerland, https://wmo.int/publication-series/wmo-global-annual-decadal-climate-update-2024-2028, 2024.

Zscheischler, J., Westra, S., Van Den Hurk, B. J., Seneviratne, S. I., Ward, P. J., Pitman, A., AghaKouchak, A., Bresch, D. N., Leonard, M., Wahl, T., et al.: Future climate risk from compound events, Nature climate change, 8, 469–477, 2018.